Operational flexibility of future generation portfolios using high spatial- and temporal-resolution wind data

Operational flexibility of future generation portfolios using high spatial- and temporal-resolution wind data

Alasdair R. W. Bruce, Jon Gibbins, Gareth P. Harrison, *Senior Member, IEEE*, Hannah Chalmers

***Abstract*—Increasing amounts of variable renewable energy sources will cause fundamental and structural changes to thermal power plant operating regimes. Maintaining key reserve requirements will lead to an increase in power plant start-ups and cycling operations for some units. An enhanced unit commitment model with energy storage and flexible CO_2 capture is formulated. High-resolution on-/offshore wind data for the UK, and probabilistic wind power forecast, model wind imbalances at operational timescales. The strategic use of flexible CO_2 capture and energy storage helps maintain reserve levels, decreasing power plant cycling operations and wind curtailment. A temporally-explicit variability assessment of net demand illustrates the generation flexibility requirements and the non-linear impacts of increasing wind capacity on power plant operating regimes.**

***Index Terms*—CO_2 capture and storage (CCS), energy storage, operational flexibility, power systems, unit commitment, wind forecasting, wind power.**

NOMENCLATURE

Indices and sets:

g	Generating unit index
s	Energy storage unit index
t	Time interval index

Decision variables:

$s_{g,t}^{\text{base}}$	Base power plant unit status
$s_{g,t}^{\text{base,start}}$, $s_{g,t}^{\text{base,shut}}$	Base power plant start-up/shut-down event
$s_{g,t}^{\text{capt}}$	CO_2 capture plant status

Variables:

C_t^{curt}	Wind curtailment cost (£)
$C_{g,t}^{\text{start}}$, $C_{g,t}^{\text{shut}}$	Start-up/shut-down costs (£)
$C_{g,t}^{\text{var}}$	Variable operating costs (£)
D_t	Electricity demand (MW)
$E_{s,t}$	Energy storage level (MWh)
$P_{g,t}^{\text{base}}$	Power output of base power plant (MW)
$P_{g,t}^{\text{capt}}$	Power demand of CO_2 capture plant (MW)
$P_{s,t}^{\text{d}}$, $P_{s,t}^{\text{c}}$	Storage discharge/charge power (MW)
R_t^{up} , R_t^{dn}	Up/down reserve requirement (MW)
$R_{g,t}^{\text{up}}$, $R_{g,t}^{\text{dn}}$	Up/down reserve contribution (MW)
$R_t^{\text{SR,up}}$, $R_t^{\text{SR,dn}}$	Up/down spinning reserve required (MW)
$R_t^{\text{StR,up}}$, $R_t^{\text{StR,dn}}$	Up/down standing reserve required (MW)
W_t	Wind generation (MW)
W_t^{curt}	Wind curtailment (MW)
$X_{g,t}$	Online(+)/offline(–) operating hours
$Y_{g,t}^{\text{capt}}$	CO_2 capture rate of CO_2 capture plant (-)
$\eta_{g,t}^{\text{base}}$	Real-time efficiency of power plant (-)
$\eta_{s,t}^{\text{rt}}$	Storage round-trip efficiency (-)
π_t	System electricity price (£/MWh)
σ_t^{D} , σ_t^{W}	Demand/wind forecast error (MW)

Parameters:

c^{CO_2}	Price of CO_2 (£/tCO_2)
c_g^{fuel}	Fuel price (£/MWh$_{\text{th}}$)
$c_g^{\text{start,cold}}$	Cold start-up cost (£)
$c_g^{\text{start,fixed}}$	Fixed start-up costs (£)
$e_g^{\text{CO}_2}$	CO_2 emission intensity (tCO_2/MWh$_{\text{th}}$)
$E_{s,\max}$	Max energy storage level (MWh)
$E_g^{\text{start,cold}}$	CO_2 emissions during cold start-up (tCO_2)
$F_g^{\text{start,cold}}$	Fuel use during cold start-up (MWh$_{\text{th}}$)
$P_{g,\max}^{\text{base}}$, $P_{g,\min}^{\text{base}}$	Max/min power output of power plant (MW)
$P_{g,\max}^{\text{capt}}$, $P_{g,\min}^{\text{capt}}$	Max/min power demand CO_2 capture (MW)
$P_g^{\text{capt,fixed}}$	Fixed power demand of CO_2 capture (MW)
$P_{s,\max}^{\text{d}}$, $P_{s,\max}^{\text{c}}$	Max discharge/charge power (MW)
$q_g^{\text{capt,op}}$	Energy to capture 1 tCO_2 (MWh/tCO_2)
$q_g^{\text{start,capt}}$	Fraction of CO_2 captured during start-up (-)
SU_g , SD_g	Start-up/shut-down time (h)

This research project is funded by the Energy Technology Partnership in Scotland, SSE plc and the University of Edinburgh.

A. R. W. Bruce, H. Chalmers, and G. P. Harrison are with the Institute for Energy Systems, School of Engineering, University of Edinburgh, Edinburgh EH9 3DW, UK (e-mail: Alasdair.Bruce@ed.ac.uk).

J. Gibbins is with the Institute for Materials and Processes, School of Engineering, University of Edinburgh, Edinburgh EH9 3FB, UK.

$UT_{g,\min}$, $DT_{g,\min}$	Minimum up/down time (h)
$Y^{\text{capt}}_{g,\max}$, $Y^{\text{capt}}_{g,\min}$	Max/min CO_2 capture rate (-)
η^{d}_s , η^{c}_s	Discharge/charge efficiency (-)
ρ^{up}_g , ρ^{dn}_g	Up/down ramp rates of power plant (MW/h)
τ_s	Rate of leakage of storage unit (%/h)
τ^{c}_g	Thermal cooling time constant (h)

I. Introduction

THE proportion of electricity demand met by variable renewable energy sources (VRE) is increasing. However, their integration will fundamentally change thermal power plant operating regimes, particularly in systems with limited energy storage and interconnection, such as Great Britain (GB) [1]. Wind power, in particular, is typically price-insensitive with priority of dispatch and is characterized by near-zero variable costs, locational dependency and limited predictability [2]. While improved wind forecasting techniques are reducing wind output uncertainty, the residual uncertainty and variability will increase as the VRE capacity increases relative to dispatchable plant. High net demand variability (demand less VRE) will impact the cycling operations and start-up/shut-down schedules of thermal power plants.

Managing this variability and uncertainty in generation and demand over operational time-scales requires more flexible operation from dispatchable thermal power plants [3], energy storage [4], demand-side management and interconnection. The term operational flexibility is defined as the technical ability of an individual unit (or power system) to manage variability and uncertainty in generation and demand over operational time-scales. The technical ability of thermal power plants and energy storage units to provide flexibility is important when considering whole-system flexibility. Valuing and quantifying flexibility is an area of ongoing research [5], [6]. The typically higher ramping capabilities of energy storage units has particular value at operational time-scales. A number of studies have proposed unit commitment formulations with energy storage scheduling methods [7], [8].

Recent work has investigated the operational flexibility of commercial-scale CO_2 capture and storage (CCS) [9], [10] and the load-following capabilities of modern nuclear reactors [11]. However, low-carbon generation technologies, such as nuclear and CCS, may be designed or financed to be technically and/or commercially inflexible. Several studies have proposed unit commitment formulations with CCS equipped power plants [12], [13]. However, CCS power plants have their own operational characteristics and have the capability to respond dynamically to market prices by adjusting the CO_2 capture rate.

This paper presents a new framework for the unit commitment (UC) problem for a portfolio of energy storage units, flexible CCS-equipped power plants, and conventional thermal units to better understand the operational flexibility and non-linear characteristics of future power systems.

The paper is laid out as follows. Section II describes the use of a high spatial- and temporal-resolution wind hindcast to capture the variability and uncertainty of expected future wind output; a prerequisite for understanding generation flexibility needs. Additionally, it outlines modelling of the stochastic and temporal correlation elements of wind forecast errors. Section III outlines the UC formulation necessary for a comprehensive analysis of power plant cycling operations, dynamic CO_2 capture plant operation and energy storage. To enable focus on the impacts on generation requirements, the operational security of the transmission network is not considered, although it is accepted that transmission constraints play an important role in power system operation. Section IV uses an illustrative set of generation portfolios to assess the power plant characteristics and operational requirements for system costs and power plant cycling. The results highlight important questions about the flexibility requirements of low-carbon electricity systems with CCS.

II. Wind Modeling

Characterization of the variability and uncertainty of the wind resource is a pre-requisite to understanding the needs for operational flexibility in future power systems. Many power system studies extrapolate wind speed measurements from meteorological masts to evaluate the impacts of wind variability [1]. More recent studies, however, utilize publically available reanalysis data to produce moderate spatial resolution wind speed datasets [14] [15]. In this work a high spatial- and temporal-resolution wind hindcast is applied [16].

A. Wind Power Time Series

The capabilities of the state-of-the-art Weather Research and Forecasting (WRF) mesoscale numerical weather prediction system [17] enabled Hawkins [16] to develop an hourly hindcast of on- and offshore wind speeds for the British Isles. Covering the years 2000 to 2010, the 3km spatial resolution allows the model to accurately simulate wind power outputs at existing and potential sites. The dataset has been extensively validated so no additional detail is presented here; a complete description of the dataset can be found in [16]. It has been applied in a range of other work including [18].

Locations of 386 existing and proposed wind sites are selected from the UK Wind Energy Database [19]. These are understood to provide a good representation of future wind deployment and will therefore credibly capture the effects of spatial distribution on the operation of future generation portfolios. Hourly wind speed and wind directionality measurements are extracted from the hindcast dataset at 337 onshore and 49 offshore locations.

The output of a wind farm is smoother than that of an individual turbine. Credible estimates of wind farm production are created using aggregate power curves that represent the smoothing effect influenced by the site dimensions and the turbulence intensity. This work follows the methodology in [1], [15], [20] by convolving the power curve for a single wind turbine with a normal distribution function (Fig. 2). The variance of the distribution is estimated from turbulence intensities derived from roughness factors, wind propagation times and typical use of land [15]. Hourly wind speed time-

series for each on- and offshore wind site is converted into hourly capacity factors by selecting the value on the aggregate power curves corresponding to the wind speed. These are further aggregated into regions according to distribution network operator boundaries.

An important feature of this work is the use of historical demand data to preserve the relationship with wind. Hourly GB demand data is taken from [21] and weather-corrected to account for Average Cold Spell Winter Peak conditions.

For flexibility assessments, wind ramping is key to defining the flexibility requirements and it is therefore important that simulated wind power data correctly models observations at operational time-scales. Wind ramps are the rate of change in wind power output over a given time period. Fig. 3 shows a plot of the simulated 1-h wind ramps derived from the wind hindcast and observed wind output data for 2010 from [22]. It indicates that small inter-hourly changes in wind production are relatively common, with larger changes much less frequent.

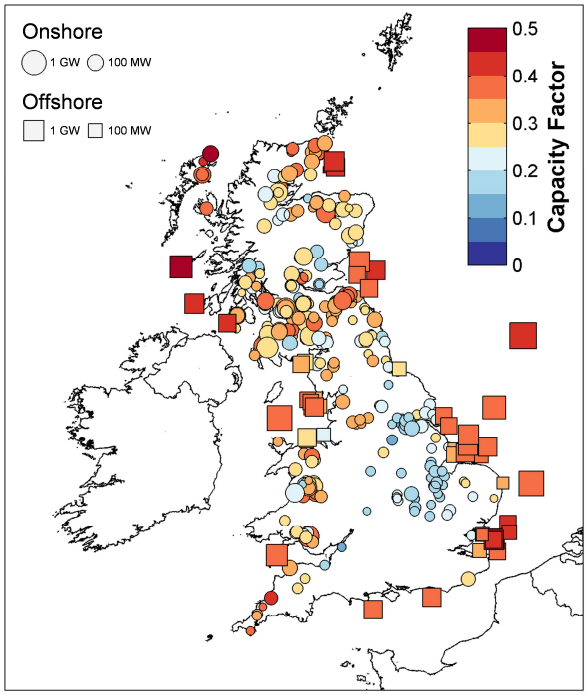

Fig. 1. The locations of onshore and offshore wind farms in the wind hindcast and the simulated long-term capacity factor 2000 to 2010.

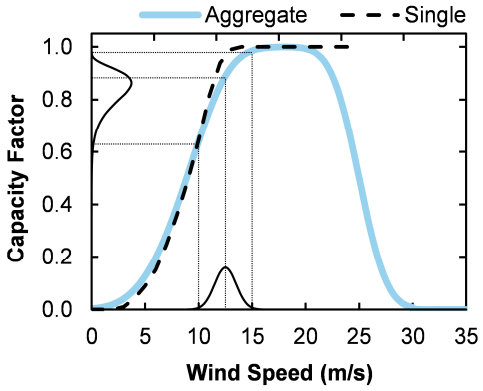

Fig. 2. Power curve for a single turbine aggregated to wind farm level.

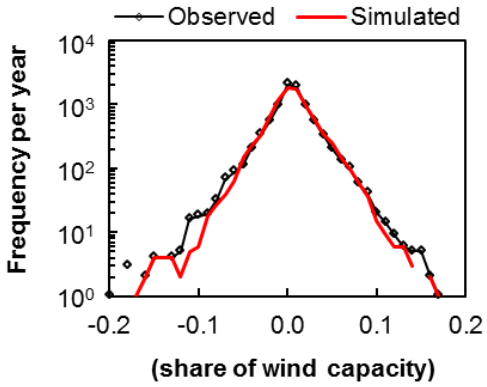

Fig. 3. Distributions for simulated and observed 1-h wind production ramp events for GB (2010 wind year).

B. *Wind Power Forecast Error*

The wind forecast error is a key consideration in operating a wind dominated power system. For a single turbine or farm, wind speed forecast errors are amplified by the non-linear power curve, translating into a more dispersed power forecast distribution (Fig. 2). For a large geographically diverse portfolio of wind farms, power forecast errors can be modelled as normally distributed random variables with zero-mean [23], [24]. A stochastic differential equation models the error distribution and correlation between forecasting periods to simulate the wind power forecast error, as described in [23]. The *realized* wind power output W_t^{r} at time t gives the *forecast* wind power output W_t^{f} and simulated wind forecast error ΔW_t according to:

$$W_t^{\mathrm{f}} = W_t^{\mathrm{r}} + \Delta W_t \quad (1)$$

An autocorrelation function models the temporal correlation in errors between forecasting periods and is approximated as an exponentially decreasing function with increasing time lag [23], i.e. a short intervals have stronger correlation.

III. Model Formulation

The analysis relies on a unit commitment (UC) framework enhanced with an integrated energy storage optimization model and a dynamic model of a flexible CCS plant with post-combustion capture. The model has both UC and economic dispatch stages to account for the change in forecast and realized wind output between the time when UC decisions are made and delivery time. At the UC stage, the operating schedules of price-sensitive energy storage units are optimized, with thermal and CCS-equipped power plants then scheduled ahead of time to supply *forecast* net demand and meet system reserve constraints. Economic dispatch is then used at delivery time to adjust the charging/discharging profiles of energy storage units and the outputs of committed thermal and CCS plants to balance *realized* net demand.

A dynamic programming solution in MATLAB is used that considers multiple predecessors, overcoming the traditional drawbacks of dynamic programming [25]. A year-long hourly analysis executes in ~18 h on an Intel Core i5 2.60 GHz processor. The solution is modified to include flexible CCS-equipped power plants increasing run times by ~10%.

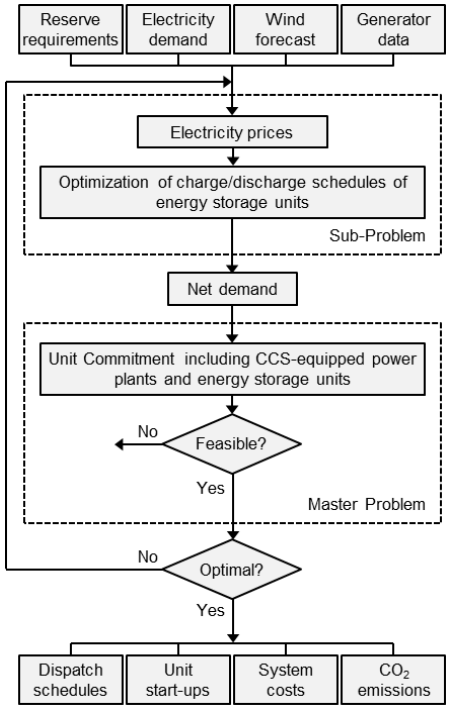

Fig. 4. Structure of the unit commitment optimization problem.

A. Unit Commitment Model

The UC minimizes total system operational costs subject to system and unit-specific operating constraints. The objective function minimizes variable operating, start-up, shut-down, and curtailment costs of the thermal generation portfolio:

$$C^{\text{total}} = \min \sum_{t=1}^{T} \sum_{g=1}^{G} C_{g,t}^{\text{var}} + C_{g,t}^{\text{start}} + C_{g,t}^{\text{shut}} + C_{t}^{\text{curt}} \quad (2)$$

where C^{total} are the total system operating costs, $C_{g,t}^{\text{start}}$ are the start-up costs, $C_{g,t}^{\text{shut}}$ are the shut-down costs, C_{t}^{curt} are the costs of onshore/offshore wind curtailment and $C_{g,t}^{\text{var}}$ are the variable operating costs that represent the no-load and variable costs of fuel, CO_2 and variable operation and maintenance (O&M, additional O&M costs apply to the CO_2 capture plant). The operating cost of onshore and offshore wind is assumed to be zero. A cost for wind curtailment is included for two reasons: firstly to avoid numerical infeasibilities during extreme low net demand periods; and secondly to account for the opportunity cost either theoretically or to compensate for lost energy and/or subsidy payments. The operating costs of energy storage units are assumed to be zero [26] therefore the UC objective function does not consider them. A piece-wise linear approximation is used to represent convex cost functions.

The operation of energy storage units is included indirectly in the UC process as the units are modelled as merchant operators seeking to maximize arbitrage revenue (alternatives include reserve provision). Storage unit schedules are optimized using forecast market prices using the same method as for economic dispatch (Section III.B) but with forecast generation. The charge/discharge profiles of the storage units are then incorporated into the forecast net demand that the UC seeks to meet. This process requires the two stage optimization shown in Fig. 4.

The system and unit specific constraints are as follows:

1) System demand balance:

$$\sum_{g=1}^{G}\left(P_{g,t}^{\text{base}} - P_{g,t}^{\text{capt}}\right) + \sum_{s=1}^{S} P_{s,t}^{\text{d}} + W_t = D_t + \sum_{s=1}^{S} P_{s,t}^{\text{c}} + W_t^{\text{curt}} \quad (3)$$

where $P_{g,t}^{\text{base}}$ and $P_{g,t}^{\text{capt}}$ are the instantaneous power outputs of the base and CO_2 capture units, $P_{s,t}^{\text{c}}$ and $P_{s,t}^{\text{d}}$ are the charge/discharging power outputs of energy storage units, W_t is onshore and offshore wind generation, and W_t^{curt} is curtailed wind generation.

2) System reserve requirements:

$$\sum_{g=1}^{G}\left(P_{g,\max}^{\text{base}} - P_{g,\min}^{\text{capt}}\right) + \sum_{s=1}^{S} P_{s,t}^{\text{d}} + W_t \geq D_t + \sum_{s=1}^{S} P_{s,t}^{\text{c}} + W_t^{\text{curt}} + R_t^{\text{up}} \quad (4)$$

$$\sum_{g=1}^{G}\left(P_{g,\min}^{\text{base}} - P_{g,\max}^{\text{capt}}\right) + \sum_{s=1}^{S} P_{s,t}^{\text{d}} + W_t \leq D_t + \sum_{s=1}^{S} P_{s,t}^{\text{c}} + W_t^{\text{curt}} - R_t^{\text{dn}} \quad (5)$$

where $P_{g,\max}^{\text{base}}$, $P_{g,\min}^{\text{base}}$, $P_{g,\max}^{\text{capt}}$ and $P_{g,\min}^{\text{capt}}$ are the maximum and minimum power outputs of the base and capture units, respectively. R_t^{up} and R_t^{dn} are the upwards and downwards system reserve requirements.

3) Unit operational status, start-up and shut-down:

$$s_{g,t}^{\text{base}} = s_{g,t-1}^{\text{base}} + s_{g,t}^{\text{base,start}} - s_{g,t}^{\text{base,shut}} \quad (6)$$

where the binary decision variables $s_{g,t}^{\text{base}}$, $s_{g,t}^{\text{base,start}}$ and $s_{g,t}^{\text{base,shut}} \in \{[0,1]$ respectively represent the operational state and start-up and shut-down events of the base power plant.

4) Unit power output constraints:

$$P_{g,\min}^{\text{base}} s_{g,t}^{\text{base}} \leq P_{g,t}^{\text{base}} \leq P_{g,\max}^{\text{base}} s_{g,t}^{\text{base}} \quad (7)$$

$$P_{g,\min}^{\text{capt}} s_{g,t}^{\text{capt}} \leq P_{g,t}^{\text{capt}} \leq P_{g,\max}^{\text{capt}} s_{g,t}^{\text{capt}} \quad (8)$$

where $P_{g,\max}^{\text{base}}$ and $P_{g,\min}^{\text{base}}$ are the maximum and minimum power output limits.

5) Unit ramping constraints:

$$P_{g,t}^{\text{base}} - P_{g,t-1}^{\text{base}} + s_{g,t-1}^{\text{base}}(P_{g,\min}^{\text{base}} - \rho_g^{\text{up}}) + s_{g,t}^{\text{base}}(P_{g,\max}^{\text{base}} - P_{g,\min}^{\text{base}}) \leq P_{g,\max}^{\text{base}} \quad (9)$$

$$P_{g,t-1}^{\text{base}} - P_{g,t}^{\text{base}} + s_{g,t}^{\text{base}}(P_{g,\min}^{\text{base}} - \rho_g^{\text{dn}}) + s_{g,t-1}^{\text{base}}(P_{g,\max}^{\text{base}} - P_{g,\min}^{\text{base}}) \leq P_{g,\max}^{\text{base}} \quad (10)$$

where ρ_g^{up}, ρ_g^{dn} are the respective up and down ramp rates. An illustration of the ramping trajectories and unit constraints for a thermal power plant is shown in Fig. 5.

6) Unit minimum up/down time constraints:

$$\left(X_{g,t-1} - UT_{g,\min}\right) \cdot \left(s_{g,t-1}^{\text{base}} - s_{g,t}^{\text{base}}\right) \geq 0 \quad (11)$$

$$\left(-X_{g,t-1} - DT_{g,\min}\right) \cdot \left(s_{g,t}^{\text{base}} - s_{g,t-1}^{\text{base}}\right) \geq 0 \quad (12)$$

where $X_{g,t}$ is the number of hours unit g has been online(+)/ offline(–), and $UT_{g,\min}$, $DT_{g,\min}$ the minimum up and down time, which include start-up SU_g and shut-down SD_g times.

B. Economic Dispatch Model

Economic dispatch is used at delivery time to adjust the outputs of committed thermal and CCS plants and the charging/discharging profiles of energy storage units to balance *realized* net demand. This effectively simulates the balancing market and is understood to be a reasonable approximation to the GB market (although it omits the impact

of transmission constraints). The system marginal price π_t is simulated for each time step by finding the intersection between net demand and the marginal cost of the price-setting plant plus an uplift function that considers the time-weighted average start-up/shut-down costs. All generation facilities participate at each time step and non-generation costs are not considered. A similar process provides forecast market prices for the energy storage optimization at the UC stage.

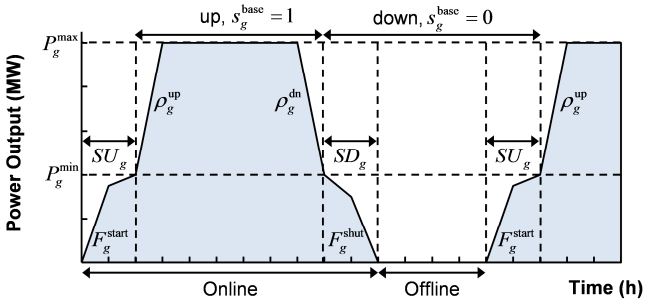

Fig. 5. Ramping trajectories and fuel consumption during start-up/shut-down.

C. Energy Storage Model

The purpose of the energy storage model is to determine the potential of time-shifting energy across a range of wind and flexibility scenarios. A Monte Carlo based optimization algorithm finds the optimal operating strategy for a portfolio of energy storage units over the optimization time horizon, in this case 168 hours. It operates both at the UC and economic dispatch stages, maximizes the operating profits of each unit, and minimizes time-dependent energy losses subject to unit-specific constraints. The operation of energy storage units (specifically the charge/discharge profiles) depend on the availability of stored energy so are formulated differently from thermal power plants. It is assumed that energy storage units only have costs associated with storing energy (i.e. purchase price of electricity) since operating and start-up/shut-down costs are typically near-zero. The objective function is:

$$\Pi_s = \max \sum_{t=1}^{T} \left(P_{s,t}^{\text{d}} - P_{s,t}^{\text{c}} \right) \cdot \pi_t \qquad (13)$$

where Π_s are the operating profits of unit s, $P_{s,t}^{\text{d}}$ is the discharging power output, $P_{s,t}^{\text{c}}$ is the charging power input, and π_t is the system electricity price. The time-dependent round-trip efficiency between time periods t_1 and t_2 is:

$$\eta_s^{\text{rt}}(\Delta t) = \eta_s^{\text{c}} \eta_s^{\text{d}} \exp\left((t_1 - t_2) / \tau_s \right) \qquad (14)$$

where $\Delta t = t_1 - t_2$, τ_s is a parameter that represents the rate of leakage, and η_s^{c} and η_s^{d} are the charging and discharging efficiencies, respectively.

Energy storage units operate when it is profitable to do so. They charge in period t_1 and discharge in period t_2, if the ratio of the respective electricity prices exceeds the inverse round-trip efficiency:

$$\pi_{t_1} / \pi_{t_2} \geq 1 / \eta_s^{\text{rt}}(\Delta t) \qquad (15)$$

Energy storage units are subject to operational constraints on charging, discharging and storage, see Fig. 6. In addition, synchronized energy storage units can rapidly adjust their charging and discharging rates and so can contribute towards the upwards and downwards spinning reserve requirements.

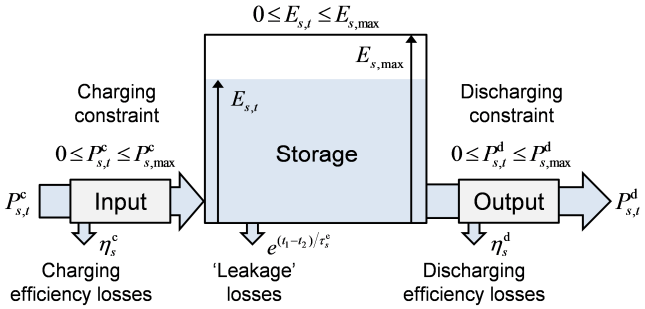

Fig. 6. Energy storage conversion characteristics.

D. Flexible CO_2 Capture Model

Incorporating CCS into the UC requires an additional binary decision variable $s_{g,t}^{\text{capt}} \in \{[0,1]$ to represent the operational status of the CO_2 capture systems (absorption, stripping and compression, Fig. 7). The base thermal power plant retains a binary variable describing its operational state.

Post-combustion CO_2 capture (PCC) with amine scrubbing is used as a representative capture technology because of its relative maturity and suitability for retrofit [27]. A flexible PCC CO_2 capture plant can rapidly redirect steam from the reboiler to the low pressure (LP) turbine to generate additional electricity [28]. It is assumed there is sufficient LP turbine flexibility to accommodate the steam flow. These CCS-equipped units can therefore temporarily reduce the steam entering the reboiler, and provide primary frequency response for up to 30 seconds and upwards spinning reserve [29]. This reduces the spinning reserve and response services that are needed from other sources. Solvent storage tanks could be installed to minimize exhaust gas venting during bypass, start-up and shut-down procedures.

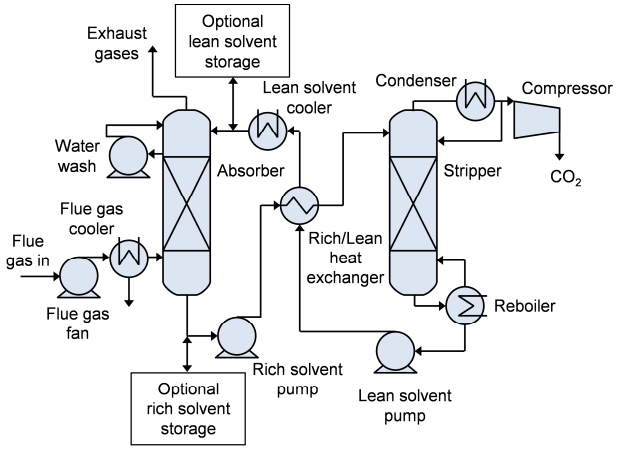

Fig. 7. Schematic of post-combustion CO_2 capture and compression systems.

CCS power plants are expected to have faster ramp rates than conventional plants since the power consumption of the capture plant can be adjusted in addition to ramping the base power plant. The operating range of CCS power plants is also larger because of lower minimum power output limits. The net power output of the CCS power plant is:

$$P_{g,t}^{\text{CCS}} = P_{g,t}^{\text{base}} - P_{g,t}^{\text{capt}} \qquad (16)$$

where $P_{g,t}^{\text{capt}}$ is the power consumption of the capture plant, specifically the loss of generation from steam extraction and to power compression and ancillary equipment [27]. To reduce modelling complexity, power consumption is modelled as a fixed component $P_g^{\text{capt,fixed}}$ and a variable component proportional to the amount of CO_2 being treated:

$$P_{g,t}^{\text{capt}} = P_g^{\text{capt,fixed}} + q_g^{\text{capt,op}} \left(P_{g,t}^{\text{base}} \eta_{g,t}^{\text{base}} e_g^{\text{CO}_2} Y_{g,t}^{\text{capt}} \right) \quad (17)$$

where $q_g^{\text{capt,op}}$ is the power consumption required to capture 1 tCO_2, $\eta_{g,t}^{\text{base}}$ is the real-time efficiency of the base power plant, $e_g^{\text{CO}_2}$ is the unit-specific CO_2 emission intensity of the base power plant and $Y_{g,t}^{\text{capt}}$ the CO_2 capture rate, which can vary between $Y_{g,\min}^{\text{capt}} \le Y_{g,t}^{\text{capt}} \le Y_{g,\max}^{\text{capt}}$. The power consumption range of a CO_2 capture plant is therefore:

$$P_{g,\max}^{\text{capt}} = P_g^{\text{capt,fixed}} + q_g^{\text{capt,op}} \left(P_{g,t}^{\text{base}} \eta_{g,t}^{\text{base}} e_g^{\text{CO}_2} Y_{g,\max}^{\text{capt}} \right) \quad (18)$$

$$P_{g,\min}^{\text{capt}} = P_g^{\text{capt,fixed}} + q_g^{\text{capt,op}} \left(P_{g,t}^{\text{base}} \eta_{g,t}^{\text{base}} e_g^{\text{CO}_2} Y_{g,\min}^{\text{capt}} \right) \quad (19)$$

E. Reserve Requirements

Upward reserve μ_t^{up} is required to cover the largest credible loss in generation (largest synchronized thermal or discharging energy storage unit), an increase in demand or decrease in wind generation to 3 standard deviations (3σ) or 99.73% of events [23], [24]. Downward reserve μ_t^{dn} is required to cover the largest credible loss in demand (largest charging energy storage unit), a decrease in demand or an increase in wind generation to 3σ. The upwards/downwards reserve requirements can be supplied from a mixture of spinning (SR) and standing reserve (StR).

$$R_t^{\text{up}} \le R_t^{\text{SR,up}} + R_t^{\text{StR,up}} = \mu_t^{\text{up}} + 3\sqrt{\left(\sigma_t^{\text{D}}\right)^2 + \left(\sigma_t^{\text{W}}\right)^2} \quad (20)$$

$$R_t^{\text{dn}} \le R_t^{\text{SR,dn}} + R_t^{\text{StR,dn}} = \mu_t^{\text{dn}} + 3\sqrt{\left(\sigma_t^{\text{D}}\right)^2 + \left(\sigma_t^{\text{W}}\right)^2} \quad (21)$$

Wind is curtailed to ensure there are a minimum number of synchronized thermal units to maintain spinning reserve, inertia and ramping requirements. This ensures minimum generation requirements for baseload power plants and ensures that constraints such as minimum stable generation limits and minimum up times are not violated. Onshore wind is curtailed before offshore wind since the constraint prices are assumed to be lower, reflecting subsidy levels [30]. Wind that is scheduled to be curtailed can contribute towards the upwards reserve requirement as curtailment suggests available energy is spilled [31]; it is calculated as the difference between forecast wind and curtailed wind. If the scheduled wind is less than $3\sigma_t^{\text{W}}$ then the reserve requirements are likely too high; the upwards reserve requirement in (20) then becomes:

$$R_t^{\text{up}} \le \mu_t^{\text{up}} + \sqrt{\left(3\sigma_t^{\text{D}}\right)^2 + \min\left(3\sigma_t^{\text{W}}, W_t^{\text{f}} - W_t^{\text{c}}\right)^2} \quad (22)$$

Demand forecast uncertainty is represented as a normally distributed function with a standard deviation σ_t^{D} of 1% of demand with zero-mean. Wind forecast errors are represented as a zero-mean normally distributed function with a standard deviation σ_t^{W} of 10% of forecast wind output 4-h ahead of real-time.

This work assumes that the upwards and downwards reserve requirement is provided by spinning reserve. This is in order to examine the impacts of flexible CO_2 capture and energy storage on reserve requirements and operational flexibility. The spinning reserve contributions from CCS-equipped power plants are limited by power output and ramp rate constraints of the base power plant:

$$R_{g,t}^{\text{up}} = \min\left(P_{g,\max}^{\text{base}} - P_{g,t}^{\text{base}}, \rho_g^{\text{up}} \Delta t\right) s_{g,t}^{\text{base}} + \left(P_{g,t}^{\text{capt}} - P_{g,\min}^{\text{capt}}\right) s_{g,t}^{\text{capt}} \quad (23)$$

$$R_{g,t}^{\text{dn}} = \min\left(P_{g,t}^{\text{base}} - P_{g,\min}^{\text{base}}, \rho_g^{\text{dn}} \Delta t\right) s_{g,t}^{\text{base}} + \left(P_{g,\max}^{\text{capt}} - P_{g,t}^{\text{capt}}\right) s_{g,t}^{\text{capt}} \quad (24)$$

F. Start-up and Shut-down

It is important to use start-up cost functions that accurately represent the dynamic non-linear costs associated with starting up a thermal power plant after a period of cooling, which depends exponentially on the number of hours spent shut-down $X_{g,t}$. The time-dependent start-up costs for thermal units equipped with/without CO_2 capture are formulated as:

$$C_{g,t}^{\text{start}} = c_g^{\text{start,cold}} \cdot \left(1 - \exp\left(X_{g,t} / \tau_g^{\text{c}}\right)\right) \quad (25)$$

$$c_g^{\text{start,cold}} = c_g^{\text{start,fixed}} + F_g^{\text{start,cold}} c_g^{\text{fuel}} + E_g^{\text{start,cold}} c^{\text{CO}_2} \left(1 - Y_{g,\max}^{\text{capt}} q_g^{\text{start,capt}}\right) \quad (26)$$

where $c_g^{\text{start,fixed}}$ represents the fixed start-up costs, τ_g^{c} is the thermal cooling time constant, $F_g^{\text{start,cold}}$ is the fuel consumption during start-up, c_g^{fuel} is the cost of fuel, $E_g^{\text{start,cold}}$ are the CO_2 emissions during a cold start-up, and c^{CO_2} is the cost of CO_2. For CCS units, $q_g^{\text{start,capt}}$ is the fraction of CO_2 that can be captured during start-up, which depends primarily on the availability and quality of steam during start-up. To enable high CO_2 capture an auxiliary boiler could provide steam prior to start-up or solvent storage tanks could be installed, if economically desirable.

IV. Case Study

A. Wind Deployment Scenarios

Several future UK wind capacity scenarios are considered to represent the expected spatial distribution and growth of the GB wind fleet into the future. The proportions of on- and offshore wind capacity are shown in Table I with offshore wind categorized into rounds for commercial development: Rounds 1 to 3 and projects in Scottish Territorial Waters (STW). Fig. 8 shows the spatial distribution of wind capacity in each of the future deployment scenarios for GB. The case study uses the 2010 wind year as the basis for analysis.

Fig. 9 shows the temporal distribution of net demand ramp events as a share of peak demand with 30 GW of wind capacity. The rate of change in net demand over 4-h timescales is a good indication of generation flexibility requirements. Upwards ramping requirements are dominated by the morning pickup, which is likely to be provided by dedicated and slower ramping thermal power plants.

TABLE I
Wind Deployment Scenarios

Wind	Onshore	Offshore			
		Round1	Round2	Round3	STW
GW	%	%	%	%	%
15	65	8	27	0	0
30	50	4	24	18	4
45	37	3	16	35	9

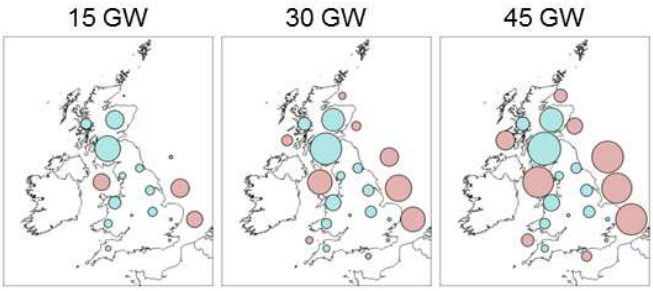

Fig. 8. Regional deployment scenarios: relative on-/offshore wind capacity.

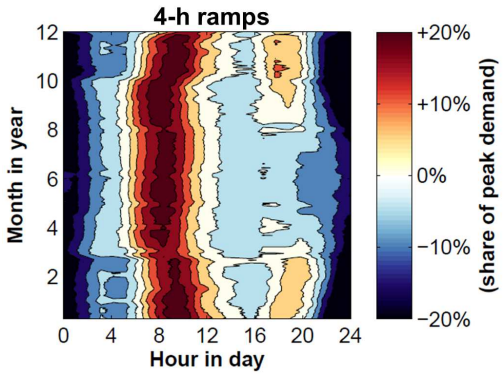

Fig. 9. Temporal distribution for 4-h net demand ramp events with 30 GW of wind capacity for GB.

B. Flexibility Scenarios

To investigate the operational flexibility of future generation portfolios with flexible CO_2 capture and energy storage, two flexibility scenarios are considered, as shown in Table II. The portfolio consists of 8 nuclear power plants, 40 combined cycle gas turbines (CCGT), 20 open cycle gas turbines (OCGT), and 4 CCGTs equipped with post-combustion capture. The technical parameters and cost characteristics of the assumed generation portfolio are based on data available in [32]. Thermal units of the same technology are modelled with varying incremental heat rates and costs to represent units of different ages and part-load efficiencies (i.e. CCGT unit 1 is more efficient than unit 40).

Fossil fuel prices are taken from the central scenarios in [33]. The CO_2 price is set at £25/tCO_2. This price is designed to reflect the anticipated low-carbon support framework in GB. The curtailment cost of on- and offshore wind are –£50/MWh and –£100/MWh, respectively.

In the low flexibility (LF) scenario, power plants have lower ramp rates and higher start-up costs. CCS-equipped power plants are not flexible and run at a constant capture rate of 90%. The PCC absorption and compression systems require 0.27 MWh_e/tCO_2 when operating at 90% capture, reducing the net electrical output at full-load to 780 MW. CCS is unable to contribute to upwards reserve and energy storage units are not included.

In the high flexibility (HF) scenario, power plants have higher ramp rates and lower start-up costs. Flexible CCS units can vary the CO_2 capture rate between zero and 90% and contribute towards upwards spinning reserve requirements. It is assumed that the CCS infrastructure does not impose additional downstream CO_2 flowrate constraints that limit operation. Four energy storage units with a total capacity of 2860 MW are included to represent the existing pumped storage capacity in the UK, see Table III. It is assumed that the operating costs of energy storage units are zero.

C. Operating Costs and CO_2 Emission Reductions

The LF scenario with 15 GW of wind capacity is treated as the base case scenario for the following comparisons. In the HF scenarios, energy storage acts as a net load and slightly increases the overall energy requirements. Nuclear power plants have lower minimum power output limits and energy storage units utilize surplus wind energy. This reduces the amount of wind curtailment leading to a significant reduction in CO_2 emissions, see Fig. 10 and Fig. 11.

During times of high electricity demand when the system marginal price is high, energy storage units discharge power and flexible CCS units increase power output by reducing the CO_2 capture rate to zero, venting CO_2 to the atmosphere. Energy storage and flexible CO_2 capture units both displace OCGT units and reduce the net spinning reserve requirements for conventional units, increasing the flexibility of the system and reducing the amount of part-loaded thermal plants. Improved thermal plant efficiencies, reduced cycling operations and curtailment reductions contribute towards system CO_2 emissions and operating cost reductions (Table IV).

For the LF 45 GW wind scenario, wind curtailment represents 15.2% of the available wind generation. Despite this, the results show that use of wind power reduces CO_2 emissions by 21.0% and 39.5% for a doubling and tripling of wind capacity, respectively. Curtailment falls to just 7.7% in the HF 45 GW scenario where the increased flexibility from nuclear units with a lower minimum stable generation limit and energy storage units are able to utilize curtailed wind. The value of energy storage and greater operational flexibility is apparent, increasing the CO_2 savings by 1.3% at 15 GW and 6.4% at 45 GW as energy storage units displace OCGT units with higher CO_2 emission intensities and wind curtailment reduces. Similar impacts are seen with system operating costs.

TABLE II
CASE STUDY GENERATION PORTFOLIO

Flexibility Scenario	Type	Units	P_{max} MW	P_{min} MW	$c_g^{start,cold}$ £/start	ρ_g MW/min
LF	Nuclear	8	1650	990	-	-
	CCGT+PCC	4	780	300	50000	5
	CCGT	40	900	360	40000	5
	OCGT	20	565	225	10000	10
HF	Nuclear	8	1650	660	-	10
	CCGT+PCC	4	875-780	335-300	25000	10
	CCGT	40	900	360	20000	10
	OCGT	20	565	225	5000	20
	Storage	4	-	-	-	-

TABLE III
ENERGY STORAGE UNIT PARAMETERS

Unit	η^{rt} %	P_{max} MW	E_{max} GWh	Duration h
1	80	1800	9.1	5.1
2	80	400	10.0	25.0
3	80	300	6.3	21.0
4	80	360	1.3	3.6

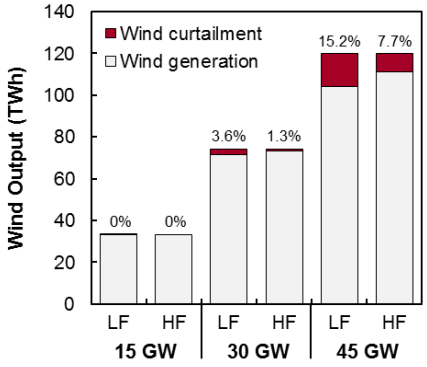

Fig. 10. Surplus wind generation with wind capacity for the low and high flexibility scenarios.

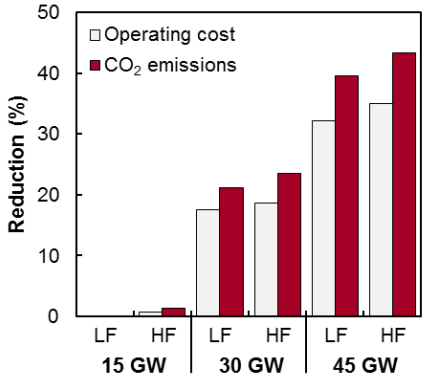

Fig. 11. Reduction in operating costs and CO_2 emissions with wind capacity for the low and high flexibility scenarios.

TABLE IV
OPERATING COSTS AND EMISSIONS

Wind	Operating cost		CO_2 emissions	
	LF	HF	LF	HF
GW	£M	£M	$MtCO_2$	$MtCO_2$
15	13066.5	12978.7	69.9	69.0
30	10779.7	10643.3	55.2	53.5
45	8855.8	8505.9	42.3	39.6

D. Thermal Plant Start-ups and Cycling Operations

CCGT units provide the majority of power system generation flexibility and ramping requirements. Fig. 12 shows how increased wind generation and varying flexibility parameters changes the CCGT ramping requirements compared to the LF 15 GW wind capacity base case scenario. In the HF scenarios energy storage units contribute towards ramping requirements, which leads to an overall reduction in CCGT ramping. Increasing wind capacity increases the magnitude and frequency of wind imbalances and displaces more efficient and traditional baseload CCGT units (1-10), forcing them to adjust output more frequently. Increasing wind generation also displaces less efficient CCGT units (11-40), which causes them to reduce output and shut-down for longer and more indeterminate periods of time.

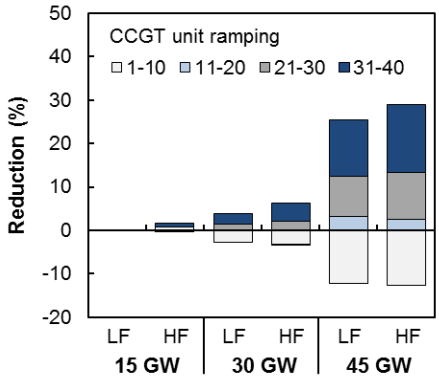

Fig. 12. Reduction in CCGT unit ramping with wind capacity for the low and high flexibility scenarios.

Fig. 13 shows the proportion of time that CCGT units spend either shut-down, at part-load or at full load for each of the scenarios. In the HF scenarios, CCGT units typically spend less time at part-load and more time at full load because increased ramp rates reduce the time required for CCGT units to adjust output between the minimum and maximum power output limits. In addition, flexible CCS and energy storage units provide upwards reserve in the HF scenarios, reducing the need for conventional CCGTs to remain at part-load and provide upwards reserve. Most CCGT units have reduced production levels with the introduction of energy storage. However, energy storage increases the baseload energy requirements for efficient CCGT units 1-10 and reduces the requirements for peaking plant and less efficient CCGT units.

Fig. 14 also shows how energy storage in the HF 15 GW and 30 GW wind scenarios increases the baseload energy requirements and therefore increases the load factors of CCS-equipped power plants. This is highly desirable for CCS units which may have to maintain stable or consistent flows of CO_2 to meet the requirements of the rest of the CCS transport, storage and injection infrastructure. Increasing the utilization of capital intensive and low carbon generation technologies is also expected to reduce the levelized cost of electricity. CCS-equipped power plants benefit from energy storage during periods of low net demand when CCS units may have to part-load or shut-down. However, energy storage and increased generation flexibility also reduces the amount of wind curtailment. Increased levels of wind generation in the HF 45 GW wind scenario significantly reduce the load factors of CCGT units equipped with PCC as this additional wind generation further displaces CCS output.

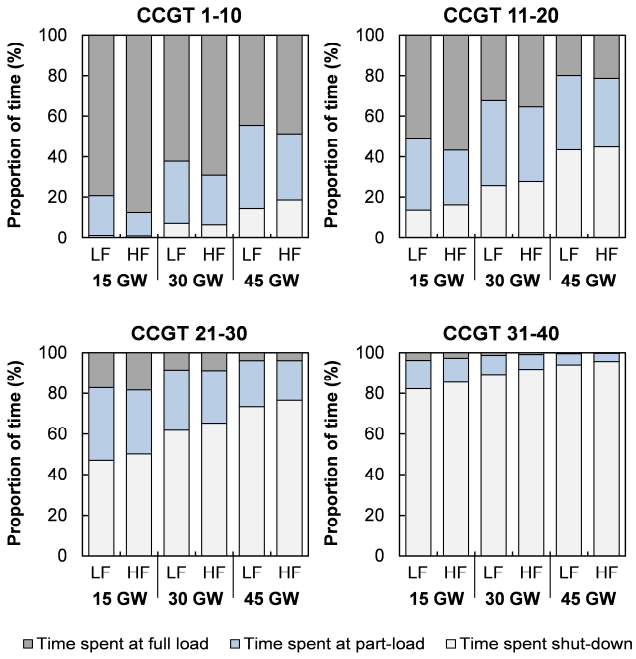

Fig. 13. Proportion of time CCGT units spend at full load, part-load, or shut-down with wind capacity for the low and high flexibility scenarios.

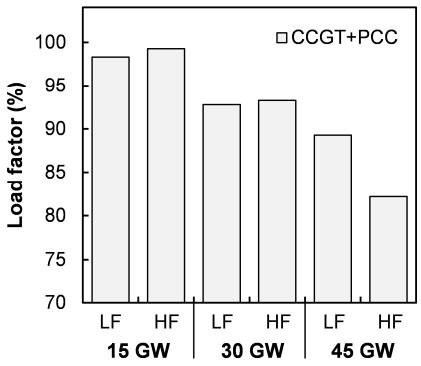

Fig. 14. Load factors of CCGT units equipped with post-combustion CO_2 capture with wind capacity for the low and high flexibility scenarios.

Fig. 15 illustrates the changing start-up requirements for CCGT units with increasing wind capacity and shows the CCGT start-ups per year categorized by the time spent shut-down for the LF and HF scenarios. The number of hours each CCGT unit spends shut-down and the number of start-ups is counted. This allows power plant start-ups to be categorized by the time spent shut-down. This gives an accurate indication of the changing hot/warm/cold start-up requirements with increasing wind capacity and the impacts of flexibility characteristics such as start-up and shut-down costs. In the HF scenarios, the number of start-ups for mid-merit CCGTs increases. This is because power plants seek to minimize the time spent at unprofitable loads making it more likely for units with lower start-up/shut-down costs to change states.

With increasing wind capacity, the start-up requirements for CCGTs changes dramatically, with a significant increase in the number of hot start-ups (where the time spent shut-down $t \leq 8$) for more efficient CCGTs with lower operating costs (units 0 to 10). For less efficient CCGTs with higher operating costs (units 20 to 40), the number of start-ups per year falls with increasing wind capacity. There is a significant increase in the number of cold start-ups for these units as they are forced to shut-down for longer periods of time. This increases the average cost and CO_2 emissions per start-up and highlights the non-linear impacts of increasing wind generation on power plant operating regimes. This result also demonstrates the importance of using time-dependent start-up cost functions that model the dynamic fuel requirements during start-ups. Furthermore, use of time-dependent start-up cost functions to capture the change in start-up requirements is necessary as any inaccuracies will impact short-term operation decisions.

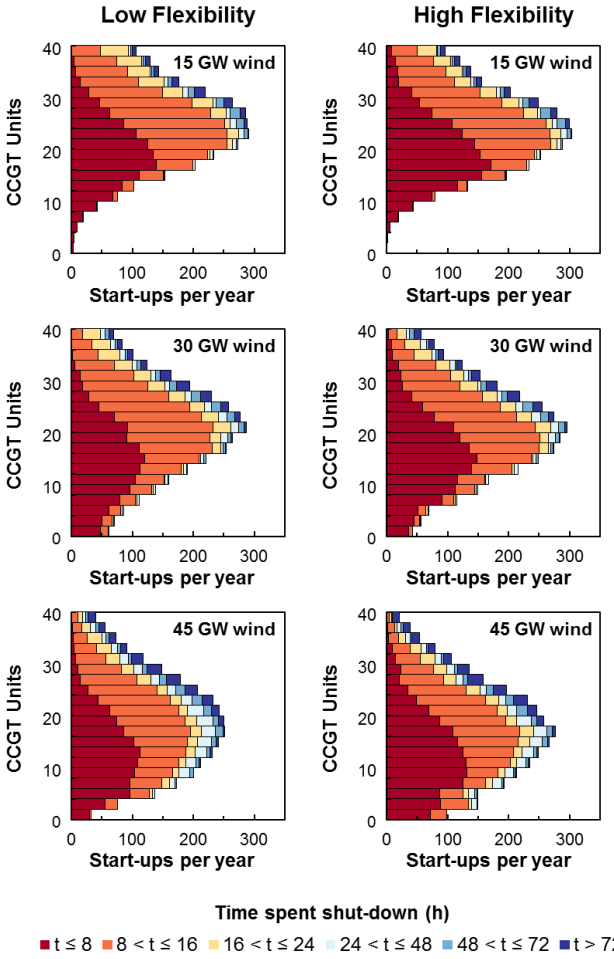

Fig. 15. Number of CCGT start-ups per year categorized by the time spent shut-down with wind capacity for the low and high flexibility scenarios

V. Conclusions

The proposed unit commitment model considers a portfolio of energy storage units, flexible CO_2 capture equipped power plants, and conventional thermal units to better understand the operational flexibility and non-linear characteristics of future power systems. An extensive wind hindcast dataset of the British Isles is used to generate high-resolution on-/offshore wind data to model wind imbalances at operational timescales. Two flexibility scenarios illustrate the impact of start-up costs and ramping capabilities on system operating costs and CO_2

emissions. Energy storage and flexible CO_2 capture units contribute towards reserve requirements and decrease the proportion of part-loaded thermal units. CCGT start-up requirements change dramatically with increasing wind deployment, highlighting the fundamental and structural changes in power plant operating regimes.

VI. Acknowledgments

This research project is funded by the Energy Technology Partnership in Scotland and SSE plc. Discussions with James Cruise from Heriot-Watt University and Ricky Chaggar at SSE plc are gratefully acknowledged.

VII. References

[1] Poyry Energy, Impact of intermittency: How wind variability could change the shape of British and Irish electricity markets [Online]. Available: http://www.poyry.co.uk/projects/intermittency

[2] I. J. Pérez-Arriaga, and C. Batlle, "Impacts of intermittent renewables on electricity generation system operation," *Economics of Energy and Environmental Policy*, vol. 1, pp. 3–17, Jan. 2012.

[3] B. C. Ummels, M. Gibescu, E. Pelgrum, W. L. Kling, and A. J. Brand, "Impacts of wind power on thermal generation unit commitment and dispatch," *IEEE Trans. Energy Convers.*, vol. 22, no. 1, pp. 44–51, Mar. 2007.

[4] C. O'Dwyer, and D. Flynn, "Using Energy Storage to Manage High Net Load Variability at Sub-Hourly Time-Scales," *IEEE Trans. Power Systems*, vol. PP, no. 99, pp. 1–10, Sep. 2014.

[5] J. Ma, V. Silva, R. Belhomme, D. S. Kirschen, and L. F. Ochoa, "Evaluating and Planning Flexibility in Sustainable Power Systems", *IEEE Trans. Sustain. Energy*, vol. 4, no. 1, pp. 200-209, Jan. 2013.

[6] E. Lannoye, D. Flynn, M. O'Malley, "Power System Flexibility Assessment - State of the Art," in *Proc. 2012 IEEE Power and Energy Soc. Gen. Meeting*, San Diego, CA, USA, pp. 1–6.

[7] D. Pozo, J. Contreras, and E. E. Sauma, "Unit Commitment With Ideal and Generic Energy Storage Units," *IEEE Trans. Power Systems*, vol. 29, no. 6, pp. 2974–2984, Nov. 2014.

[8] Y. Wen, C. Guo, H. Pandzic, and D. S. Kirschen, "Enhanced Security-Constrained Unit Commitment With Emerging Utility-Scale Energy Storage," *IEEE Trans. Power Systems*, vol. PP, no. 99, pp. 1–8, Mar. 2015.

[9] H. Chalmers, M. Leach, M. Lucquiaud, and J. Gibbins, "Valuing flexible operation of power plants with CO_2 capture," *Energy Procedia*, vol. 1, no. 1, pp. 4289–4296, Feb. 2009.

[10] S. Cohen, G. Rochelle, and M. Webber, "Optimal CO_2 capture operation in an advanced electric grid," *Energy Procedia*, vol. 37, pp. 2585–2594, Aug. 2013.

[11] NEA, Technical and Economic Aspects of Load Following with Nuclear Power Plants. [Online]. Available: http://www.oecd-nea.org/ndd/reports/2011/load-following-npp.pdf

[12] S. Lou, S. Lu, Y. Wu, and D. S. Kirschen, "Optimizing Spinning Reserve Requirement of Power System With Carbon Capture Plants," *IEEE Trans. Power Systems*, vol. 30, no. 2, pp. 1056–1063, Mar. 2015.

[13] J. Li, J. Wen, and X. Han, "Low-carbon unit commitment with intensive wind power generation and carbon capture power plant," *J. Mod. Power Syst. Clean Energy*, vol. 3, no. 1, pp. 63–71, Jan. 2015.

[14] P. Li, J. Wu, X. Guan, and Y. Zhou, "Probabilistic Forecasting of Aggregated Generation for Regional Wind Farms with Geographical Dynamic Model," in *Proc. 2012 IEEE Power and Energy Soc. Gen. Meeting*, San Diego, CA, USA, pp. 1–8.

[15] I. Staffell, and R. Green, "How does wind farm performance decline with age?" Renewable Energy, vol. 66, pp. 775–786, Jun. 2014.

[16] S. Hawkins, "A high resolution reanalysis of wind speeds over the British Isles for wind energy integration," Ph.D. Thesis, University of Edinburgh, U.K., 2012.

[17] National Center for Atmospheric Research, WRF ARW Version 3 Modeling System User's Guide [Online]. Available: http://www2.mmm.ucar.edu/wrf/users/docs/user_guide_V3.5/ARWUsersGuideV3.pdf

[18] G. P. Harrison, S. L. Hawkins, D. Eager, and L. C. Cradden, "Capacity Value of Offshore Wind in Great Britain," *Proc. IMechE, Part O: Journal of Risk and Reliability*, in press, 2015.

[19] RenewableUK, UK Wind Energy Database (UKWED) [Online]. Available: http://www.renewableuk.com/en/renewable-energy/wind-energy/uk-wind-energy-database/index.cfm

[20] P. Norgaard, and H. Holttinen, "A multi-turbine power curve approach," in *Proc. 2004 Nordic Wind Power Conference*, Chalmers University of Technology, Sweden, pp. 1–5.

[21] National Grid, 2014. Metered half-hourly electricity demands. [Online]. Available:http://www.nationalgrid.com/

[22] ELEXON, The New Electricity Trading Arrangements [Online]. Available: http://www.bmreports.com/

[23] J. Ma, "Evaluating and Planning Flexibility in a Sustainable Power System with Large Wind Penetration," Ph.D. Thesis, University of Manchester, U.K., 2012.

[24] V. Silva, "Value of flexibility in systems with large wind penetration," Ph.D. Thesis, Imperial College London, U.K., 2010.

[25] G. B. Sheble, G. N. Fahd, "Unit commitment literature synopsis," *IEEE Trans. Power Systems*, vol. 9, no. 1, pp. 128–135, Feb. 1994.

[26] H. Zhao, Y. Feng, X. Q. Zhang, Z. Ren, "Hydro-thermal unit commitment considering pumped storage stations," in *1998 IEEE International Conference on Power System Technology - (POWERCON 2012)*, Beijing, China, vol. 1, pp. 576-580.

[27] IEAGHG, 2011, Retrofitting CO_2 capture to existing power plants 2011/2 May 2011 [Online]. Available: http://ieaghg.org/docs/General_Docs/Reports/2011-02.pdf

[28] M. Lucquiaud, P. Patel, H. Chalmers, and J. Gibbins, "Retrofitting CO_2 capture ready fossil plants with post-combustion capture. Part 2: requirements for natural gas combined cycle plants using solvent-based flue gas scrubbing," in *Proc. Inst. Mech. Eng. A J. Power Energy*, vol. 223, no.3, pp. 227–238, 2009.

[29] M. R. Haines, and J. Davison, "Enhancing dynamic response of power plant with post combustion capture using 'Stripper stop'," *International Journal of Greenhouse Gas Control*, vol. 20, pp. 49–56, 2014.

[30] National Grid, 2014, Electricity Ten Year Statement 2014. [Online]. Available: http://www2.nationalgrid.com/UK/Industry-information/Future-of-Energy/Electricity-Ten-Year-Statement/

[31] J. Ma, V. Silva, L. F. Ochoa, D. S. Kirschen, R. Belhomme, "Evaluating the Profitability of Flexibility," in *Proc. 2012 IEEE Power and Energy Soc. Gen. Meeting*, San Diego, CA, USA, pp. 1–8.

[32] Parsons Brinkerhoff, Electricity Generation Cost Model - 2013 Update of Non-renewable Technologies. [Online]. Available: https://www.gov.uk/government/publications

[33] DECC, DECC Fossil Fuel Price Projections, Sep. 2014. [Online]. Available: https://www.gov.uk/government/publications

VIII. Biographies

Alasdair R. W. Bruce received the B.Sc. degree in Physics from the University of Warwick in 2010 and the M.Sc. degree in Sustainable Energy Systems from the University of Edinburgh in 2011. He is currently working toward the Ph.D. degree from the Institute for Energy Systems, University of Edinburgh, with research interests in power system flexibility and renewable integration.

Jon Gibbins received the B.Sc. degree in Mechanical Engineering from Imperial College London in 1978 and the Ph.D. degree in Chemical Engineering from Imperial College London in 1988. He is currently Professor in Power Plant Engineering and Carbon Capture at the University of Edinburgh with research interests in carbon capture and storage and both coal and biomass gasification and combustion.

Gareth P. Harrison (M'02 SM'14) is Bert Whittington Chair of Electrical Power Engineering at the University of Edinburgh, Edinburgh, U.K. His current research interests include network integration of renewable generation and analysis of the impact of climate change on the electricity industry. Prof. Harrison is a Chartered Engineer and member of the Institution of Engineering and Technology, U.K.

Hannah Chalmers received the M.Eng. degree in Mechanical Engineering from Imperial College London in 2006, a Diploma of Imperial College in Mechanical Engineering and Energy Policy in 2010, and the Ph.D. degree in Environmental Strategy from the University of Surrey in 2010. She is currently a Senior Lecturer in Power Plant Engineering at the University of Edinburgh with research interests in power plant and CO_2 capture engineering.